J Geod (2010) 84:705–714
DOI 10.1007/s00190-010-0404-4

ORIGINAL ARTICLE

Rapid re-convergences to ambiguity-fixed solutions in precise point positioning

Jianghui Geng · Xiaolin Meng · Alan H. Dodson · Maorong Ge · Felix N. Teferle

Received: 25 May 2010 / Accepted: 4 August 2010 / Published online: 14 August 2010

Abstract Integer ambiguity resolution at a single receiver can be achieved if the fractional-cycle biases are separated from the ambiguity estimates in precise point positioning (PPP). Despite the improved positioning accuracy by such integer resolution, the convergence to an ambiguity-fixed solution normally requires a few tens of minutes. Even worse, these convergences can repeatedly occur on the occasion of loss of tracking locks for many satellites if an open sky-view is not constantly available, consequently totally destroying the practicability of real-time PPP. In this study, in case of such re-convergences, we develop a method in which ionospheric delays are precisely predicted to significantly accelerate the integer ambiguity resolution. The effectiveness of this method consists in two aspects: first, wide-lane ambiguities can be rapidly resolved using the ionosphere-corrected wide-lane measurements, instead of the noisy Melbourne–Wübbena combination measurements; second, narrow-lane ambiguity resolution can be accelerated under the tight constraints derived from the ionosphere-corrected unambiguous wide-lane measurements. In the test at 90 static stations suffering from simulated total loss of tracking locks, 93.3 and 95.0% of re-convergences to wide-lane and narrow-lane ambiguity resolutions can be achieved within five epochs of 1-Hz measurements, respectively, even though the time latency for the predicted ionospheric delays is up to 180 s. In the test at a mobile van moving in a GPS-adverse environment where satellite number significantly decreases and cycle slips frequently occur, only when the predicted ionospheric delays are applied can the rate of ambiguity-fixed epochs be dramatically improved from 7.7 to 93.6% of all epochs. Therefore, this method can potentially relieve the unrealistic requirement of a continuous open sky-view by most PPP applications and improve the practicability of real-time PPP.

Keywords Precise point positioning · Ambiguity resolution · Rapid re-convergence · Predicted ionospheric delays

J. Geng (✉) · X. Meng · A. H. Dodson
Institute of Engineering Surveying and Space Geodesy, University of Nottingham, Nottingham, NG7 2TU, UK
e-mail: isxjg@nottingham.ac.uk

M. Ge
GeoForschungsZentrum Helmholtz Center, 14473 Potsdam, Germany

F. N. Teferle
Faculty of Science, Technology and Communication, University of Luxemburg, 1359 Luxemburg, Luxemburg

1 Introduction

Double-difference carrier-phase ambiguities are normally fixed to integers in precise Global Positioning System (GPS) applications. Nonetheless, undifferenced ambiguities in precise point positioning (PPP) (Zumberge et al. 1997) lose their integer properties because they absorb the fractional-cycle biases (FCBs) that originate from both receiver and satellite hardware (Geng et al. 2010a). Fortunately, these integer properties can be retrieved by correcting the float ambiguity estimates with the FCBs that are derived from a network of reference stations (Ge et al. 2008). Due to the ionosphere-free observable used in PPP, integer ambiguity resolution is performed through two sequential steps: wide-lane ambiguities are first resolved using the Melbourne–Wübbena combination observable (Melbourne 1985; Wübbena 1985) and narrow-lane ambiguities are then resolved based on the resulting integer wide-lane ambiguities (Geng et al. 2009; Laurichesse et al. 2009). Geng et al. (2010b) illustrated that ambiguity

resolution can significantly improve the positioning accuracy from decimeter to centimeter level in real-time PPP.

Nevertheless, a long convergence period to such an ambiguity-fixed solution will considerably devalue the accuracy improvement contributed by the integer resolution. According to a substantial data processing, Geng et al. (2010b) concluded that at least 10 min of measurements are required to resolve about 90% of wide-lane ambiguities, whereas over 10 min for a narrow-lane ambiguity resolution. A wide-lane ambiguity is estimated using the noisy Melbourne–Wübbena combination measurements, and thus a long observation period is required to sufficiently smooth the noise. On the other hand, rapid narrow-lane ambiguity resolution is handicapped by the imprecise pseudorange measurements which cannot sufficiently shrink the search space for the integer ambiguities suffering from a rather short wavelength of 10.7 cm (Teunissen 1996). Hence, a long observation period has to be used to average out sufficiently precise pseudorange measurements in order to derive accurate ambiguity estimates (Teunissen et al. 1997). To date, however, it is still extremely difficult to develop an effective method to accelerate these convergences.

Even worse, these long-period convergences can repeatedly occur on the occasion of loss of tracking locks for many satellites. Frequent re-convergences are common problems in industrial applications and can totally destroy the practicability of real-time PPP. As a result, a continuous open sky-view is constantly required by most PPP applications to maintain a centimeter-level positioning accuracy (Bisnath and Gao 2007). To relieve this unrealistic requirement and to improve the practicability of PPP, Banville and Langley (2009) identified the integer cycle slips caused by such lock losses through differencing between epochs, simply assuming that ionospheric delays canceled out during such differences. However, they did not perform the integer resolution on undifferenced ambiguities. On the other hand, Geng (2009) developed a method where ionospheric delays were precisely predicted to tightly constrain the narrow-lane resolution to significantly accelerate re-convergences. Encouragingly, the re-convergence periods were shortened from about 1,000 to 20 s on average with a success rate of around 90%. However, Melbourne–Wübbena combination measurements were still used to fix wide-lane ambiguities, thereby hardly guaranteeing a rapid re-convergence of only a few seconds.

In this study, we aim at improving this method to achieve rapid re-convergences to ambiguity-fixed solutions within a few epochs of 1-Hz measurements. Note that "convergence" throughout this study means "achieving an ambiguity-fixed solution". In the following, Sect. 2 details the theory of this method; Sect. 3 presents a case study at static stations, investigates the impacts of time latency on the prediction error of ionospheric delays and discusses the efficiency of rapid re-convergences; Sect. 4 presents a case study at a mobile van, investigates the performance of rapid re-convergences in a GPS-adverse environment where satellite number significantly decreases and cycle slips frequently occur, and compares the results with the network real-time kinematic (NRTK) solution; finally, Sect. 5 summarizes the main points and addresses the perspective of a wide-area PPP-RTK service supported by rapid ambiguity resolution.

2 Method

In terms of the previous section, the keys to accelerating convergences consist in both avoiding the Melbourne–Wübbena combination measurements and shrinking the search space for integer ambiguities. The volume of this search space is governed by the variance–covariance matrix of ambiguity estimates, and it approximately observes the following rule (Teunissen 1996, 1997):

$$V \propto \frac{\sigma_{\mathrm{P}}}{n\lambda} \tag{1}$$

where V is the volume of search space; σ_{P} is the precision of pseudorange or unambiguous measurements; n is the number of epochs; λ is the wavelength of carrier-phase measurements; and $\propto$ denotes a proportional relationship. To achieve rapid convergences, increasing n is unrealistic, and thus we can only diminish σ_{P} or enlarge λ. In this section, we thereby derive how to precisely predict ionospheric delays and apply these delays to accelerate both the wide-lane and narrow-lane ambiguity resolutions, then discuss the implementation of this method, and finally address the ambiguity search and validation in this study.

2.1 Precisely predict ionospheric delays

In general, GPS carrier-phase measurements on frequency $g(g = 1, 2)$ at a particular epoch for a single receiver i can be written as

$$\lambda_g \Phi_{gi}^j = \rho_i^j + \lambda_g \varphi_i^j + ct_i - ct^j + T_i^j - \frac{\kappa_i^j}{f_g^2} + \lambda_g \left(B_{gi} + B_g^j + N_{gi}^j \right) + \varepsilon_{gi}^j \tag{2}$$

where the superscript $j(j = 1, \ldots)$ denotes a satellite; Φ_{gi}^j is the carrier-phase measurement where antenna phase center corrections have been applied; λ_g is the wavelength and f_g is the frequency; c is the light speed; ρ_i^j is the geometric distance between the receiver i and the satellite j; φ_i^j is the phase wind-up correction (Wu et al. 1993); t_i and t^j are the receiver and satellite clocks, respectively; T_i^j denotes a slant tropospheric delay; $\frac{\kappa_i^j}{f_g^2}$ denotes a slant ionospheric delay; B_{gi} and B_g^j are the receiver and satellite FCBs, respectively; N_{gi}^j

denotes an integer ambiguity; finally, ε_{gi}^{j} denotes unmodeled errors including multipath effects. From Eq. 2, a wide-lane measurement at this epoch can be formed as

$$\lambda_w \Phi_{wi}^{j} = \frac{\kappa_i^j}{f_1 f_2} + \rho_i^j + ct_i - ct^j + T_i^j + \lambda_w \left(B_{wi} + B_w^j + N_{wi}^j \right) + \varepsilon_{wi}^j \quad (3)$$

where λ_w is the wide-lane wavelength of about 86 cm; $\Phi_{wi}^{j} = \Phi_{1i}^{j} - \Phi_{2i}^{j}$, $B_{wi} = B_{1i} - B_{2i}$, $B_w^j = B_1^j - B_2^j$, $N_{wi}^j = N_{1i}^j - N_{2i}^j$ and $\varepsilon_{wi}^j = \frac{f_1}{f_1 - f_2}\varepsilon_{1i}^j - \frac{f_2}{f_1 - f_2}\varepsilon_{2i}^j$; and note that the phase wind-up effects on dual frequencies cancel out. In this study, Eq. 3 is hereafter used to estimate the ionospheric delay, namely the term of $\frac{\kappa_i^j}{f_1 f_2}$ in theory, at all ambiguity-fixed epochs. For a low-dynamic receiver, the ionospheric delays for each satellite normally manifest a strong temporal correlation over a few minutes (Dai et al. 2003; Kashani et al. 2007), which is the foremost foundation of our method for rapid re-convergences.

Despite this favorable characteristic of ionospheric delays, we have to further quantify the residual biases possibly assimilated into the estimate of $\frac{\kappa_i^j}{f_1 f_2}$, and investigate their temporal characteristics. First, the receiver clock seems an unstable quantity over time. Hence, a single difference between satellites j and k at this epoch can be formed, namely

$$\lambda_w \Phi_{wi}^{jk} = \frac{\kappa_i^{jk}}{f_1 f_2} + \lambda_w \left(B_w^{jk} + N_{wi}^{jk} \right) + \rho_i^{jk} - ct^{jk} + T_i^{jk} + \varepsilon_{wi}^{jk} \quad (4)$$

where the receiver clock t_i and the receiver FCB B_{wi} are consequently eliminated. The satellite FCB B_w^{jk} is normally deemed very stable over at least 24 h. Ge et al. (2008) verified this by deriving an agreement of better than 0.05 cycles between 14 days of wide-lane FCB estimates. Moreover, the integer N_{wi}^{jk} has been known in the ambiguity-fixed solution at this epoch.

Second, ρ_i^{jk} depends on both the satellite and the receiver positions. To date, predicted GPS satellite orbits by IGS over 24 h have reached an accuracy of around 5 cm (http://igscb.jpl.nasa.gov/components/prods.html) (Dow et al. 2009). Residual radial orbit errors can be mostly mitigated by satellite clocks (Senior et al. 2008), if a consistent yaw-attitude model is applied to the satellites (Kouba 2009). Moreover, GPS satellite orbits are tightly constrained by dynamic force models, and thus the residual orbit errors should change smoothly in theory. Of particular note, unannounced satellite maneuvers can significantly degrade the orbit accuracy. For the precise prediction of ionospheric delays, this can be a limiting factor, but is hereafter ignored because these maneuvers are normally rare. On the other hand, the receiver position can be known to the centimeter-level accuracy in the ambiguity-fixed solution at this epoch (Geng et al. 2010b).

Third, due to the high correlation between t^{jk} and the satellite orbits (Senior et al. 2008), favorable user range errors of centimeter level can be achieved (Hauschild and Montenbruck 2009). Nonetheless, this t^{jk} is normally a predicted value due to the communication delays in real-time applications. Fortunately, Senior et al. (2008) reported that the Rubidium and Cesium clocks on current GPS satellites can be precisely predicted to a precision of better than 0.1 ns up to a period of 40 s which covers typical communication delays. Hence, we hereafter assume that errors of satellite clocks are always smaller than 0.1 ns.

Fourth, T_i^{jk} can be mostly mitigated by estimating a zenith tropospheric delay (ZTD) based on a mapping function. Residual tropospheric delays are only a few millimeters at high elevations, but can be up to several centimeters at an elevation of smaller than 10○ (Stoew et al. 2007). However, the troposphere condition around a low-dynamic receiver slightly changes over several minutes if neither rapid weather fronts nor large height variations occur for this receiver (Gregorius and Blewitt 1999; Shan et al. 2007). Considering this similar temporal characteristic to that of ionospheric delays, we can alternatively combine the two atmospheric delays and then predict their sum over time.

Finally, ε_{wi}^{jk} is the most uncertain quantity in Eq. 4 and we believe that the multipath effect dominates among all possible unmodeled errors. Dilßner et al. (2008) showed that the carrier-phase biases caused by multipath effects stemming from solely radiating near fields can theoretically reach a few centimeters for low-elevation satellites. Although Han and Rizos (2000) described the strong temporal correlation of the multipath signatures at static antennas, such signatures can be quite random and thus unpredictable at mobile antennas.

Therefore, at an ambiguity-fixed epoch, knowing the quantities of N_{wi}^{jk}, ρ_i^{jk}, t^{jk} and T_i^{jk}, we can deduct them from Φ_{wi}^{jk} and obtain the ionospheric-delay estimate, namely

$$\hat{I}_{wi}^{jk} = \lambda_w \Phi_{wi}^{jk} - \lambda_w N_{wi}^{jk} - \hat{\rho}_i^{jk} + ct^{jk} - \hat{T}_i^{jk} = \frac{\kappa_i^{jk}}{f_1 f_2} + \lambda_w B_w^{jk} + e_{wi}^{jk} + \varepsilon_{wi}^{jk} \quad (5)$$

where $\hat{\rho}_i^{jk}$ and $\hat{T}_i^{jk}$ are the estimates of ρ_i^{jk} and T_i^{jk}, respectively, which are derived from the ambiguity-fixed solution of this epoch; e_{wi}^{jk} contains the errors of the satellite product and the tropospheric delay. According to the quantitative assessments above, we can infer that $e_{wi}^{jk} + \varepsilon_{wi}^{jk}$ can easily amount to over 10 cm for low-elevation satellites. However, B_w^{jk} changes negligibly over a long time and e_{wi}^{jk} changes minimally or predictably over a few minutes, thereby minimally affecting the temporal-correlation characteristic of

$\frac{\kappa_i^{jk}}{f_1 f_2}$. Hence, $\hat{I}_{wi}^{jk}$ can be precisely predicted to the succeeding epochs over a few minutes, especially at static antennas where multipath effects are also temporally correlated. Note that the error caused by the receiver position estimate is ignored in Eq. 5 because this error will be absorbed by the position estimate where the predicted ionospheric delays are applied (refer to Sect. 2.2). In this study, $\hat{I}_{wi}^{jk}$ is simply called "ionospheric delay" for brevity although it contains more than a true ionospheric delay.

For the predicting strategy, we suggest the linear fitting model where estimated ionospheric delays within a sliding time window are used to fit a linear function, and a predicted delay is then extrapolated using this function (Dai et al. 2003). In this study, the time gap between a predicted and the latest estimated ionospheric delays is named as the latency of this predicted delay. This time latency can be caused by data gaps, for example. The prediction error at an epoch is quantified by differencing the predicted and estimated ionospheric delays at this epoch. Geng (2009) illustrated that the prediction error is increased when the elevation angle becomes smaller and the time latency becomes longer, and this increasing rate depends on the ionosphere condition. Hence, besides the elevation-dependent weighting on the predicted ionospheric delays by Geng (2009), namely

$$p(E) = \begin{cases} 1.0 & 30^\circ \le E \le 90^\circ \\ 2\sin E & 7^\circ \le E < 30^\circ \end{cases} \tag{6}$$

where E is the elevation angle in degrees, a latency-dependent weighting is also required, such as

$$p(\tau) = \begin{cases} 1.0 & \tau < 30\ \mathrm{s} \\ \tan\left(\frac{\pi}{4} \cdot \frac{30}{\tau}\right) & \tau \ge 30\ \mathrm{s} \end{cases} \tag{7}$$

where τ is the time latency in seconds and the "30 s" will be illustrated in Sect. 3.2.

2.2 Rapidly retrieve integer ambiguities

Integer ambiguities can be rapidly retrieved by applying the above precisely predicted ionospheric delays after a re-convergence occurs. This is achieved through two steps. First, at a particular epoch where the ambiguity-fixed solution has been lost, wide-lane measurements are formed using Eq. 4 and are corrected by the known satellite products, the latest ZTD estimate, and the predicted ionospheric delays. If the time latency is shorter than a few minutes, the wide-lane-measurement errors caused by FCBs, satellite products and atmospheric delays can be canceled out or mostly mitigated by the counterparts in the predicted ionospheric delays (Dai et al. 2003; Kashani et al. 2007). Note that unmodeled errors are not easily predicted and thereby supposed to be sufficiently small in this study. Finally, we obtain

$$\lambda_w \Phi_{wi}^{jk} + c t^{jk} - \breve{T}_i^{jk} - \breve{I}_{wi}^{jk} = \rho_i^{jk} + \lambda_w N_{wi}^{jk} + \zeta_{wi}^{jk} \tag{8}$$

where $\breve{T}_i^{jk}$ is the slant tropospheric delay computed using the latest ZTD estimate that is derived from previous solutions; $\breve{I}_{wi}^{jk}$ is the predicted ionospheric delay; ζ_{wi}^{jk} contains the unmodeled errors and the prediction error of ionospheric delays, and it actually quantifies the precision of Eq. 8; moreover, only the positions and ambiguities are unknown. Constrained by the ionosphere-free pseudorange measurements, the wide-lane ambiguity N_{wi}^{jk} can be resolved using Eq. 8 if ζ_{wi}^{jk} is small enough (e.g. $\prec 1/4\lambda_w$). In terms of Eq. 1, thanks to the relatively long wavelength for wide-lane ambiguities, ionosphere-free pseudorange measurements can normally sufficiently shrink the search space to only a few integer candidates, thereby improving the search efficiency and accelerating the identification of integer ambiguities.

Second, at this epoch, once the wide-lane ambiguity is successfully resolved, Eq. 8 becomes a precise unambiguous measurement, namely

$$\lambda_w \Phi_{wi}^{jk} + c t^{jk} - \breve{T}_i^{jk} - \breve{I}_{wi}^{jk} - \lambda_w N_{wi}^{jk} = \rho_i^{jk} + \zeta_{wi}^{jk} \tag{9}$$

In this study, it is Eq. 9, rather than the pseudorange measurements, that is superimposed to the normal equation of PPP and thus constrains the integer identification of narrow-lane ambiguities during rapid re-convergences. In terms of Eq. 1, if the magnitude of ζ_{wi}^{jk} is far smaller than a few centimeters, applying Eq. 9 can considerably shrink the search space for narrow-lane ambiguities to a few integer candidates. As a result, narrow-lane ambiguity resolution can be accelerated. Note that the prediction error of ionospheric delays dominates ζ_{wi}^{jk} if the time latency is long. An imprecisely predicted ionospheric delay will weaken the constraint imposed by Eq. 9, possibly failing a rapid re-convergence.

Finally, we stress that both rapid resolutions above minimally rely on the satellite-geometry change, but on the sufficient shrink of search space for integer candidates. Such shrinks are achieved by applying the ionosphere-free pseudorange and the ionosphere-corrected unambiguous wide-lane measurements which are precise enough relative to the wide-lane and narrow-lane wavelengths, respectively. As a result, float ambiguity estimates are close to the correct integers and these integers can then be relatively easily identified, even though only one epoch of measurements is used.

2.3 Remarks on the method implementation

From the method described above, the prerequisite of this method is how to precisely predict ionospheric delays, which depends on three aspects:

- Temporal properties of all errors in the ionospheric-delay estimate by Eq. 5. Although the true ionospheric delay dominates its temporal variation, other errors including

clock predictions and multipath effects should also be carefully regarded;

- Predicting strategy. Currently, it is not easy to precisely predict the ionosphere condition over a long time due to its complicated relationships with the geomagnetic field, the solar activity, etc. especially during an ionospheric storm. For example, sudden ionospheric disturbances and scintillations may occur during high ionosphere activities in polar and equatorial regions (Basu et al. 2002). As a result, temporal ionospheric irregularities cannot be precisely depicted beforehand in real-time applications. In this case, only the linear trend of the ionosphere variation can usually be quantified with a relatively high confidence level (Dai et al. 2003). However, we should keep in mind that the residual variations can sometimes be very large and thus fail the precise prediction of ionospheric delays;
- Model consistency between the ionospheric-delay estimation using Eq. 5 and the wide-lane ambiguity resolution using Eq.8. Note that both models are derived from Eq.4. In this manner, their common biases can naturally cancel out without impairing the integer ambiguities, hence explaining why we do not care about the biases assimilated into the estimated ionospheric delays, but their prediction errors.

Heretofore, we need to acknowledge that this method applies to only re-convergences because ionospheric delays are estimated only at ambiguity-fixed epochs as demonstrated in Sect. 2.1. Nonetheless, if a dense network of reference stations is available, ionospheric delays can also be estimated at the reference stations and then interpolated at single users to assist rapid convergences. In this case, the first ambiguity-fixed solution can also be rapidly achieved.

2.4 Ambiguity search and validation

For the ambiguity search, we used the least-squares ambiguity decorrelation adjustment method (Teunissen 1995) to search for integer candidates. All available satellites over an elevation angle of 7° were used for wide-lane ambiguity resolution, whereas those over 15° for narrow-lane ambiguity resolution (Geng et al. 2009).

For the ambiguity validation, the ratio test, where the ratio of the second minimum to the minimum quadratic form of residuals is assessed, was used with a threshold of 2 which was adopted by many authors (e.g. Teunissen and Verhagen 2009; Wang et al. 1998). Of particular note, however, a fixed threshold here is not reasonable in theory because it should vary with the strength of the underlying GPS model and the degrees of freedom (Teunissen and Verhagen 2009). In this case, an improved ratio test or GPS model may potentially improve the efficiency of ambiguity resolution, thus possibly further accelerating the convergences (Verhagen and Teunissen 2006; Wang et al. 1998, 2002). However, these issues are beyond the scope of this study and thus ignored throughout.

3 A case study at static stations

In this section, we investigate the prediction error of ionospheric delays, and assess this method at static stations by quantifying the success rate of rapid re-convergences and the time spent on achieving the ambiguity-fixed solution.

3.1 Data processing

Seven days of 24-h 1-Hz GPS data from July 6–12 in 2008 at about 90 stations across Europe were collected from the European Reference Frame—Internet Protocol project (Bruyninx 2004) and the Ordnance Survey of Great Britain real-time network (Fig. 1). The Kp index, which quantifies the ionosphere-activity level, was below 4 on average, thus showing a moderate ionosphere condition. At these stations, positions were estimated as white noise at each epoch, and ZTDs were estimated every three hours. To test rapid re-convergences, we introduced a total signal interruption 20 min after each successful convergence, and thus each station suffered from about 70 re-convergences per day if there were no large data gaps. After each total signal interruption, a number of epochs of measurements were removed to simulate a time latency for the predicted ionospheric delays. This dataset is quite representative for the mid-latitude regions during moderate ionosphere conditions because it covers 24 h per day and contains receivers working in different environments.

In addition, the IGS predicted orbits and Earth rotation parameters were used. The satellite clock and FCB determination refer to Geng (2009) and Geng et al. (2010b) (see

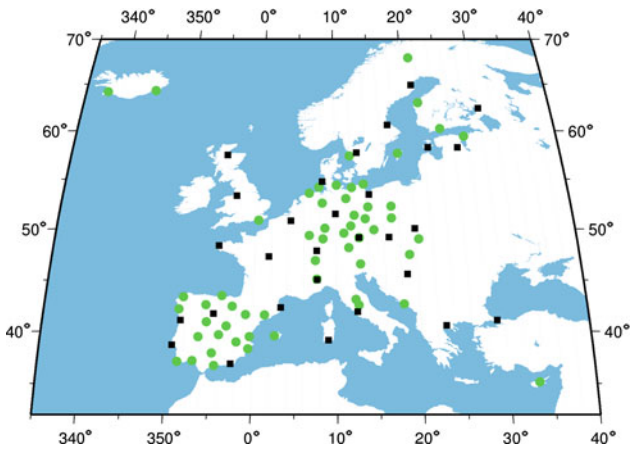

Fig. 1 Distribution of 1-Hz stations across Europe among which *black solid squares* denote the stations used for real-time satellite clock and FCB determination

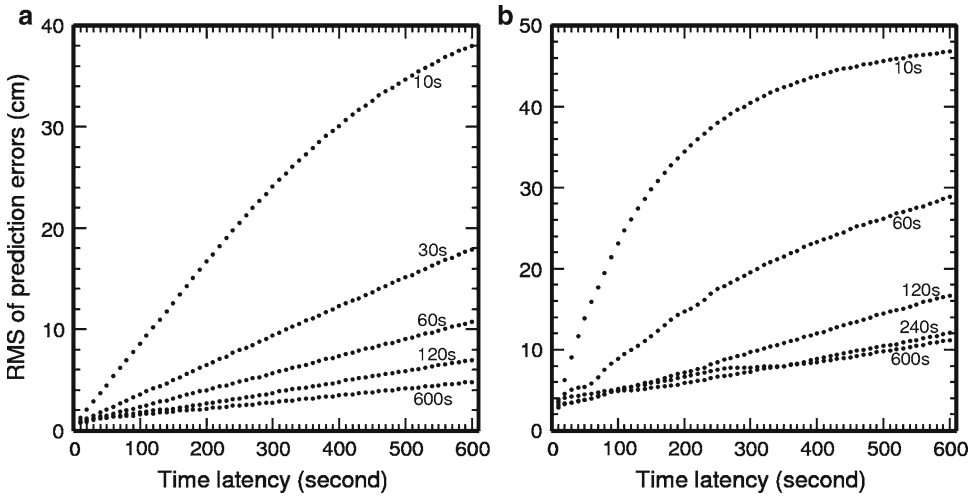

Fig. 2 RMS of the prediction errors of ionospheric delays under different time window widths which are labeled alongside the solid circles, different time latencies and different elevation angles: (a) >30° and (b) ≤30°

Fig. 1), and communication delays were ignored in this simulated real-time study. These also apply to the case study in Sect. 4.

3.2 Prediction error of ionospheric delays

The prediction error of ionospheric delays is subject to both the time latency and the elevation angle. In Fig. 2, the ionospheric delays at a typical station ACOR are divided into two groups using an elevation angle of 30°. The RMS of their prediction errors for all satellite pairs during 24 h is plotted against both the time latency and the time window width. As expected, the RMS is increased when the time latency is prolonged. However, enlarging the window width can slow down this increasing rate. Because a large window width degrades the computation efficiency, we finally choose 120 s as a trade-off for the ionospheric delays above 30° and 240 s for those below 30° in this study. In this case, the error for a 300-s prediction is only 3.7 cm for the ionospheric delays over 30° and 7.3 cm for those below 30°. In addition, the prediction error remains steady when the time latency is shorter than 30 s, thus explaining why identical weights are posed within 30 s in Eq. 7.

3.3 Performance of rapid re-convergences

Applying the precisely predicted ionospheric delays can significantly improve the success rate of rapid re-convergences and shorten the time spent on these re-convergences. Table 1 shows the statistics about the rapid re-convergences achieved within five epochs of 1-Hz measurements under different time latencies. When the time latency is 10 s, 99.4 and 98.7% of re-convergences to wide-lane and narrow-lane ambiguity resolutions can be rapidly achieved, respectively. Even though the time latency is up to 180 s, these two percentages can still reach 93.3 and 95.0%. For comparison, if we do not apply the precisely predicted ionospheric delays, only 78.9% of all re-convergences can be achieved within 20 minutes with a mean time of 694 s. Hence, the improvement on the re-convergence efficiency by this method is encouragingly significant.

However, when the time latency is up to 300 s, the above two percentages steadily fall to 85.8 and 89.4%. This deterioration can be understood in terms of the amplified prediction-error of ionospheric delays. From Eq. 8, ionospheric delays of large prediction errors will enlarge the magnitude of ζ_{wi}^{jk}, hence possibly biasing the corresponding wide-lane ambiguity estimates and degrading the reliability of integer resolutions. Furthermore, even though a rapid wide-lane ambiguity resolution can be achieved, a large ζ_{wi}^{jk} will lead to a poor precision of an unambiguous measurement by Eq. 9, hence weakening the resulting constraint on the subsequent narrow-lane ambiguity resolution. Finally, when the time latency is only 10 s, the failure rates for the wide-lane and narrow-lane resolutions account for 0.6 and 1.3%, respectively, most of which are caused by low satellite availability and poor satellite geometry.

On the other hand, Table 1 also shows the mean times to resolve wide-lane and narrow-lane ambiguities. When the time latency is 10 s, only one epoch of data is required to resolve wide-lane ambiguities, whereas almost no more epochs are required to resolve narrow-lane ambiguities. Overall, increasing the time latency will lead to a longer time spent on achieving the ambiguity-fixed solution. However, these times are increased moderately or even minimally, implying that most rapid re-convergences are achieved using only one epoch of measurements, even though the time latency is up to 300 s. In fact, this finding demonstrates that the satellite-geometry change minimally contributes to the rapid re-convergences in this study.

Table 1 Performance of rapid re-convergences within five epochs of 1-Hz measurements under different time latencies

Time latency (s)	Wide-lane ambiguity resolution		Narrow-lane ambiguity resolution	
	Success rate (%)	Time to fix (s)	Success rate (%)	Time to fix (s)
10	36459/36665 (99.4)	1.00	36159/36618 (98.7)	0.02
30	35236/35822 (98.4)	1.01	35223/35720 (98.6)	0.02
60	33782/34632 (97.5)	1.02	33860/34472 (98.2)	0.03
120	31003/32333 (95.9)	1.03	31011/32060 (96.7)	0.05
180	28060/30070 (93.3)	1.05	28024/29500 (95.0)	0.09
240	25134/28024 (89.7)	1.10	25058/27088 (92.5)	0.12
300	22417/26137 (85.8)	1.17	21875/24465 (89.4)	0.15

A "success rate" is the ratio (*within parentheses*) between the number (*before slashes*) of rapid resolutions and the total number (*behind slashes*) of resolutions for the wide-lane or narrow-lane ambiguities. A "time to fix" is the real-valued mean of all times spent on resolving the wide-lane or narrow-lane ambiguities. Note that one second here represents one epoch of measurements, and the time to fix a narrow-lane ambiguity begins to be measured when the corresponding wide-lane ambiguity is successfully resolved

4 A case study at a mobile van

In this section, we assess this method at a van moving in a GPS-adverse environment, then interpolate ionospheric delays based on a dense reference network and finally compare the results with those from a commercial NRTK service.

4.1 Data processing

A van-borne 1-Hz GPS data set was collected in the city of Nottingham on May 11, 2009, covering about 2.5 h from 11:30 to 14:04 (Local time). The Kp index was around 1 during this period, showing a quiet ionosphere condition. As shown in Fig. 3, the van stopped or moved in four phases: (1) it stopped from 11:40 to 12:27 on a car park with an open sky view; (2) it moved from 12:27 to 13:12 along the red routes escorted by tall buildings, large trucks and thick trees; (3) it stopped again from 13:12 to 13:44 on the car park; (4) finally, it moved again from 13:44 to 14:04 along the blue routes on the car park with a few thick trees around. A reference station was located on top of the IESSG building which was within 2 km from the van. Moreover, this reference station was surrounded by other six reference stations within a distance from about 50–100 km (upper inset). They were used to interpolate ionospheric and tropospheric delays. In addition, the lower inset shows the satellite number which kept steady during the stopping phases, but changed dramatically during the moving phases due to signal obstructions.

At this van, because the antenna's attitudes during the moving phases were unknown, we applied the phase wind-up corrections by assuming that the antenna's rotation was always around its boresight. In this case, the phase wind-up effects caused by this rotation can be fully assimilated into the receiver clock without affecting the correction proposed by Wu et al. (1993) (Banville and Langley 2009). Moreover, no antenna phase center corrections were applied. We estimated

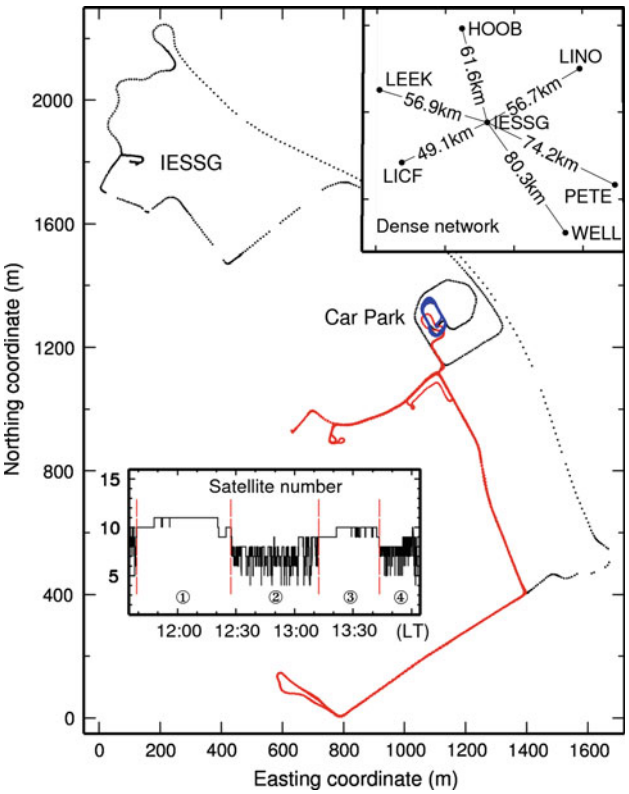

Fig. 3 Van trajectory consisting of four phases: (1) it stopped on the car park with an open sky view; (2) it moved along the red routes escorted by tall buildings, large trucks and thick trees; (3) it stopped again on the car park; (4) it moved along the blue routes on the car park with a few thick trees around. A reference station was located at IESSG. The *upper inset* shows the distances between six reference stations and IESSG, whereas the *lower inset* shows the satellite number and the time spans for the four phases. "LT" denotes local time

only one ZTD during this experiment because the time span was short and the area was small. A ground truth was computed using the Leica Geo Office software of version 3.0 and the IESSG station was used as reference. We believe that the

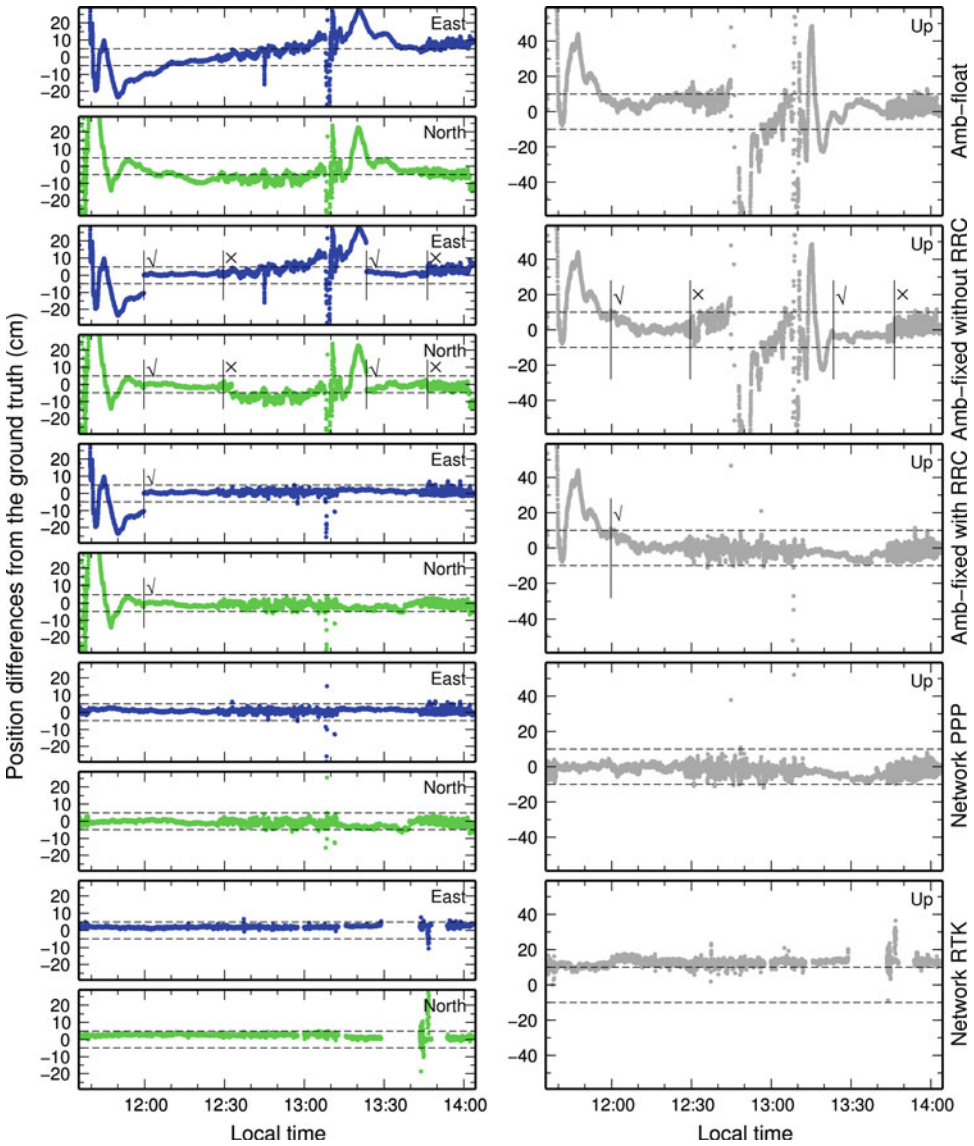

Fig. 4 Position differences from the ground truth that is derived from a post-processed short-baseline solution for the East, North and Up components. From top to bottom show the ambiguity-float solution, the ambiguity-fixed solutions without and with rapid re-convergences (RRC), the ambiguity-fixed solution supported by a dense network (network PPP) and the network RTK solution. The symbol "√" denotes the time when the ambiguity-fixed solution is achieved, whereas "×" denotes the time when the ambiguity-fixed solution is totally lost

3D accuracy of this ground truth should be better than a few centimeters. In addition, an NRTK solution provided by the Leica SmartNet service was also collected for comparison.

4.2 Rapid convergences in a GPS-adverse environment

In a GPS-adverse environment, frequent and severe signal obstructions can significantly jeopardize the positioning performance and the ambiguity resolution. In Fig. 4, for the ambiguity-float solutions, a clear trend is present for the East component and a bias for the North component. During the first moving phase when signals were frequently obstructed, all three components, especially vertical, experience large position errors of over a few decimeters. If the ambiguities are resolved, the positioning accuracy can be clearly improved for all three components, but this improvement is present only during the stopping phases as shown in Fig. 4. Ambiguity-fixed solutions were quickly and totally lost after the moving phases began. This is because re-convergences occurred due to the signal obstructions. Overall, the rate of ambiguity-fixed epochs is only 7.7% of all epochs during the moving phases.

Nevertheless, by further applying our method for rapid re-convergences, ambiguity-fixed solutions can be well maintained during the moving phases. From Fig. 4, the accuracies of both horizontal components during the moving phases are better than 5 cm, whereas that of vertical is better than 10 cm. Large position errors are present at only a few epochs where ambiguity-fixed solutions cannot be achieved. More encouragingly, the rate of ambiguity-fixed epochs is significantly increased to 93.6% of all epochs during the moving phases, showing a significant improvement over the ambiguity-fixed solutions without rapid re-convergences.

Nevertheless, the first ambiguity-fixed solution is achieved after a few tens of minutes. To solve this problem, the six surrounding reference stations were used to interpolate the

ionospheric delays at this van. As a result, only five epochs of 1-Hz measurements are used to achieve the first ambiguity-fixed solution. Moreover, the epochs with large position errors become much fewer. Actually, the rate of ambiguity-fixed epochs reaches up to 97.2% of all epochs during the moving phases. This further improvement is largely attributed to the interpolated ionospheric delays which are more reliable than the predicted ones.

4.3 Comparisons with an NRTK solution

Normally, a NRTK service can generate centimeter-level positioning accuracy using double-difference measurements based on an RTK network. At the bottom of Fig. 4, we present the position differences of an NRTK solution against the ground truth. Note that the gaps are caused by the unavailability of NRTK correction messages. Large position errors occur from 13:40 to 13:50, and thus are excluded from the following statistics. It can be clearly seen that biases are present for all three components, especially for the Up one. We believe that these biases are largely caused by the antenna phase center corrections applied to the NRTK solution. Disregarding these discrepancies, we find that the ambiguity-fixed solutions enhanced by rapid convergences perform comparably with the NRTK solution. Specifically, the standard deviations of the differences for the East, North and Up components during the moving phases are 1.0, 1.3 and 2.7 cm for the ambiguity-fixed solutions with rapid re-convergences, respectively, whereas 0.6, 1.0 and 1.4 cm for the NRTK solution.

Nonetheless, from Fig. 4, the position differences during the moving phases for the NRTK solution scatter clearly more tightly than those of the ambiguity-fixed PPP solutions enhanced by rapid convergences. On the contrary, the position differences during the stopping phases for all these solutions scatter comparably. This hence demonstrates that the internal consistency between the ground truth and the NRTK solution due to the software similarity cannot adequately explain the distinct scatters during the moving phases. Therefore, we argue that this issue might be because the phase wind-up corrections cannot be precisely computed during the moving phases, since the antenna's true attitudes were unknown.

5 Conclusions and perspective

In this study, we develop a method where the ionospheric delays are predicted to the succeeding epochs to accelerate the ambiguity resolution in case of re-convergences. In theory, the effectiveness of this method consists in two aspects: on the one hand, wide-lane ambiguities can be rapidly resolved using the ionosphere-corrected wide-lane measurements, instead of the noisy Melbourne–Wübbena combination measurements; on the other hand, narrow-lane ambiguities can be rapidly resolved under the tight constraints derived from the ionosphere-corrected unambiguous wide-lane measurements.

This method is verified using two tests under moderate ionosphere conditions. At static stations suffering from simulated total losses of tracking locks, even if the time latency for the predicted ionospheric delays is up to 180 s, 93.3 and 95.0% of re-convergences to wide-lane and narrow-lane ambiguity resolutions can be achieved within five epochs of 1-Hz measurements, respectively. If this time latency is prolonged, the prediction error of ionospheric delays is increased, consequently reducing both percentages above. On the other hand, for most rapid re-convergences, only one epoch of measurements is needed, implying that the contribution of satellite-geometry changes to these rapid re-convergences is minimal in this study. At a mobile van moving in a GPS-adverse environment, ambiguity-fixed solutions can be well maintained when rapid re-convergences are applied. The rate of ambiguity-fixed epochs is significantly improved from 7.7 to 93.6% of all epochs during the moving phases. Additionally, the RMS of position differences from the ground truth that is derived from a post-processed short-baseline solution are 1.0, 1.3 and 2.7 cm for the East, North and Up components, respectively, which are comparable with those of the NRTK solution.

Finally, the ionospheric delays can also be interpolated from a dense network of reference stations. Although such networks are normally not available for PPP, we can envision that if precise ionospheric delays can be derived from a sparse network at scales of several hundred kilometers using an ionospheric tomography technique (e.g. Hernández-Pajares et al. 2000), a PPP-RTK service (Geng et al. 2010b) that can rapidly provide ambiguity-fixed solutions may potentially prevail against current RTK positioning services based on dense networks.

Acknowledgments This study is based on an improved Positioning and Navigation Data Analyst (PANDA) software package which was originally developed by Wuhan University in China (Shi et al. 2008). The authors thank the IGS, the European Reference Frame—Internet Protocol project and the Ordnance Survey of Great Britain for the data provision. The authors also thank the editor and three anonymous reviewers whose constructive comments and suggestions significantly improve the paper quality.

References

Banville S, Langley RB (2009) Improving real-time kinematic PPP with instantaneous cycle-slip correction. In: Proceedings of ION

GNSS 22nd international technical meeting of the satellite division, Savannah, US, pp 2470–2478
Basu S, Groves KM, Basu Su, Sultan PJ (2002) Specification and forecasting of scintillations in communication/navigation links: current status and future plans. J Atmos Sol-Terr Phys 64(16): 1745–1754
Bisnath S, Gao Y (2007) Current state of precise point positioning and future prospects and limitations. In: Sideris MG (ed) Observing our changing Earth. Springer, New York, pp 615–623
Bruyninx C (2004) The EUREF Permanent Network: a multi-disciplinary network serving surveyors as well as scientists. GeoInformatics 7:32–35
Dai L, Wang J, Rizos C, Han S (2003) Predicting atmospheric biases for real-time ambiguity resolution in GPS/GLONASS reference station networks. J Geod 76(11–12):617–628
Dilßner F, Seeber G, Wübbena G, Schmitz M (2008) Impact of near-field effects on the GNSS position solution. In: Proceedings of ION GNSS 21st International Technical Meeting of the Satellite Division, Savannah, US, pp 612-624
Dow JM, Neilan RE, Rizos C (2009) The International GNSS Service in a changing landscape of Global Navigation Satellite Systems. J Geod 83(3–4):191–198
Ge M, Gendt G, Rothacher M, Shi C, Liu J (2008) Resolution of GPS carrier-phase ambiguities in precise point positioning (PPP) with daily observations. J Geod 82(7):389–399
Geng J (2009) Rapid re-convergence in real-time precise point positioning with ambiguity resolution. In: Proceedings of ION GNSS 22nd international technical meeting of the satellite division, Savannah, US, pp 2437–2448
Geng J, Teferle FN, Shi C, Meng X, Dodson AH, Liu J (2009) Ambiguity resolution in precise point positioning with hourly data. GPS Solut 13(4):263–270
Geng J, Meng X, Dodson AH, Teferle FN (2010a) Integer ambiguity resolution in precise point positioning: method comparison. J Geod. doi:10.1007/s00190-010-0399-x
Geng J, Teferle FN, Meng X, Dodson AH (2010b) Towards PPP-RTK: ambiguity resolution in real-time precise point positioning. Adv Space Res. doi:10.1016/j.asr.2010.03.030
Gregorius TLH, Blewitt G (1999) Modeling weather fronts to improve GPS heights: a new tool for GPS meteorology?. J Geophys Res 104(B7):15261–15279
Han S, Rizos C (2000) GPS multipath mitigation using FIR filters. Surv Rev 35(277):487–498
Hauschild A, Montenbruck O (2009) Kalman-filter-based GPS clock estimation for near real-time positioning. GPS Solut 13(3):173–182
Hernández-Pajares M, Juan JM, Sanz J, Colombo OL (2000) Application of ionospheric tomography to real-time GPS carrier-phase ambiguities resolution, at scales of 400-1000 km and with high geomagnetic activity. Geophys Res Lett 27(13):2009–2012
Kashani I, Wielgosz P, Grejner-Brzezinska D (2007) The impact of the ionospheric correction latency on long-baseline instantaneous kinematic GPS positioning. Surv Rev 39(305):238–251
Kouba J (2009) A simplified yaw-attitude model for eclipsing GPS satellites. GPS Solut 13(1):1–12
Laurichesse D, Mercier F, Berthias JP, Broca P, Cerri L (2009) Integer ambiguity resolution on undifferenced GPS phase measurements and its application to PPP and satellite precise orbit determination. Navig J Inst Navig 56(2):135–149
Melbourne WG (1985) The case for ranging in GPS-based geodetic systems. In: Proceedings of first international symposium on precise positioning with the global positioning system, US, pp 373–386
Senior KL, Ray JR, Beard RL (2008) Characterization of periodic variations in the GPS satellite clocks. GPS Solut 12(3):211–225
Shan S, Bevis M, Kendrick E, Mader GL, Raleigh D, Hudnut K, Sartori M, Phillips D (2007) Kinematic GPS solutions for aircraft trajectories: identifying and minimizing systematic height errors associated with atmospheric propagation delays. Geophys Res Lett 34:L23S07. doi:10.1029/2007GL030889
Shi C, Zhao Q, Geng J, Lou Y, Ge M, Liu J (2008) Recent development of PANDA software in GNSS data processing. In: Proceedings of the society of photographic instrumentation engineers, 7285:72851S doi:10.1117/12.816261
Stoew B, Nilsson T, Elgered G, Jarlemark POJ (2007) Temporal correlation of atmospheric mapping function errors in GPS estimation. J Geod 81(5):311–323
Teunissen PJG (1995) The least-squares ambiguity decorrelation adjustment: a method for fast GPS integer ambiguity estimation. J Geod 70(1–2):65–82
Teunissen PJG (1996) An analytical study of ambiguity decorrelation using dual frequency code and carrier phase. J Geod 70(8):515–528
Teunissen PJG (1997) On the sensitivity of the location, size and shape of the GPS ambiguity search space to certain changes in the stochastic model. J Geod 71(9):541–551
Teunissen PJG, de Jonge PJ, Tiberius CCJM (1997) The least-squares ambiguity decorrelation adjustment: its performance on short GPS baselines and short observation spans. J Geod 71(10):589–602
Teunissen PJG, Verhagen S (2009) The GNSS ambiguity ratio-test revisited: a better way of using it. Surv Rev 41(312):138–151
Verhagen S, Teunissen PJG (2006) New global navigation satellite system ambiguity resolution method compared to existing approaches. J Guid Control Dynam 29(4):981–991
Wang J, Stewart MP, Tsakiri M (1998) A discrimination test procedure for ambiguity resolution on-the-fly. J Geod 72(11):644–653
Wang J, Satirapod C, Rizos C (2002) Stochastic assessment of GPS carrier phase measurements for precise static relative positioning. J Geod 76(2):95–104
Wu JT, Wu SC, Hajj GA, Bertiger WI, Lichten SM (1993) Effects of antenna orientation on GPS carrier phase. Manuscr Geod 18(2):91–98
Wübbena G (1985) Software developments for geodetic positioning with GPS using TI-4100 code and carrier measurements. In: Proceedings of first international symposium on precise positioning with the global positioning system, US, pp 403–412
Zumberge JF, Heflin MB, Jefferson DC, Watkins MM, Webb FH (1997) Precise point positioning for the efficient and robust analysis of GPS data from large networks. J Geophys Res 102(B3):5005–5017